Bulletin of the New Zealand Society for Earthquake Engineering, Vol. 51, No. 2, June 2018

PASSIVE DIRECTION DISPLACEMENT DEPENDENT DAMPING (D3) DEVICE

Nikoo K. Hazaveh[1], Geoffrey W. Rodgers[2], J. Geoffrey Chase[3] and Stefano Pampanin[4]

(Submitted *April 2017*; Reviewed *July 2017*; Accepted *November 2017*)

ABSTRACT

Viscous fluid damping has been used worldwide to provide energy dissipation to structures during earthquakes. Semi-active dissipation devices have also shown significant potential to re-shape structural hysteresis behaviour and thus provide significant response and damage reduction. However, semi-active devices are far more complex and costly than passive devices, and thus potentially less robust over time. Ideally, a passive device design would provide the unique response behaviour of a semi-active device, but in a far more robust and low-cost device. This study presents the design, development and characterization of a passive Direction and Displacement Dependent viscous damping (D3) device. It can provide viscous damping in any single quadrant of the force-displacement hysteresis loop and any two in combination. Previously, this behaviour could only be obtained with a semi-active device. The D3 device is developed from a typical viscous damper, which is tested to evaluate the baseline of orifice sizing, force levels and velocity dependence. This prototype viscous damper is then modified in clear steps to produce a device with the desired single quadrant hysteresis loop. The overall results provide the design approach, device characterization and validation for this novel device design.

INTRODUCTION

Several studies have demonstrated the effectiveness of semi-active dissipation for enhancing seismic performance, attaining safety levels not easily achieved in conventional structures using current design criteria [1-10]. The potential of many classes of semi-active devices and control methods, including variable stiffness and variable damping, to mitigate damage during seismic events is well-documented [1-3,5,7,9,10].

Many prior semi-active devices have been air or fluid based systems based on the principles of variable stiffness [3,8,9,11], but were complex and could not produce the very large control forces often required for controlling realistic structures. To address this problem, Hazaveh et al. [12-15] evaluated the concept of semi-active viscous dampers and examined three types of device control laws (a 1-4, 1-3 and 2-4) to sculpt hysteretic behaviour based on Chase et al. [3]. Figure 1 shows schematic hysteresis loops for a linear structure with semi-active 1-4, 1-3 and 2-4 devices, to illustrate the overall outcome of these different configurations.

The 2-4 control law appeared to be an appealing solution for reducing seismic response in displacement (structural damage) and base shear (foundation damage) by providing damping in second and forth quadrants of the hysteresis loop [11,15]. Moreover, Hezaveh et al. evaluated the performance of the 2-4 control law in a nonlinear two story structure subjected to shake table test of a half scale two-story steel frame that showed the 2-4 device could improve the structural performance without increasing base shear [16].

However, semi-active devices are far more complex and costly than passive devices, require an external power source and competition, and thus are potentially much less robust. Hence, this study first focuses on evaluating the characteristics of classic, very simple oil based viscous damper. This classic viscous damper is then modified in distinct steps to obtain a prototype viscous device with customized hysteretic response. In particular, it is modified to provide direction dependent and displacement dependent damping. The goal is to obtain a passive device design that can produce damping in any one quadrant of the hysteresis loop. In combination, two such devices could then create a passive version of the 1-3 and 2-4 semi-active devices. Experimental validation and characterization of a prototype D3 device with 30-60kN force capacity is undertaken using an MTS-810 hydraulic test machine.

MODELLING AND EVALUATION APPROACH OF A STANDARD VISCOUS DAMPER

A viscous damping device was produced with grips for testing a 100kN capacity MTS hydraulic test. General purpose Castrol Axle EPX 80W-90 oil was chosen as the fluid to be used. This fluid was selected as a very low-cost and easily accessible option, while expected the fluid has a kinematic viscosity of approximately 140mm^2/s (140cSt) at 40°C to provide reasonable force at the expected flow rate. A more expensive fluid option, such as silicone fluid could be used, but this study is intended to provide proof of concept validation of the device design, particularly at low cost, rather than a final, fluid-specific result.

[1] *Corresponding Author, PhD student, University of Canterbury, Christchurch, nikoo.hazaveh@pg.canterbury.ac.nz (Member)*
[2] *Associate Professor, University of Canterbury, Christchurch, (Member)*
[3] *Distinguished Professor, University of Canterbury, Christchurch, (Member).*
[4] *Professor, University of Canterbury, Christchurch; Professor, Sapienza University of Rome, Italy, (Fellow).*

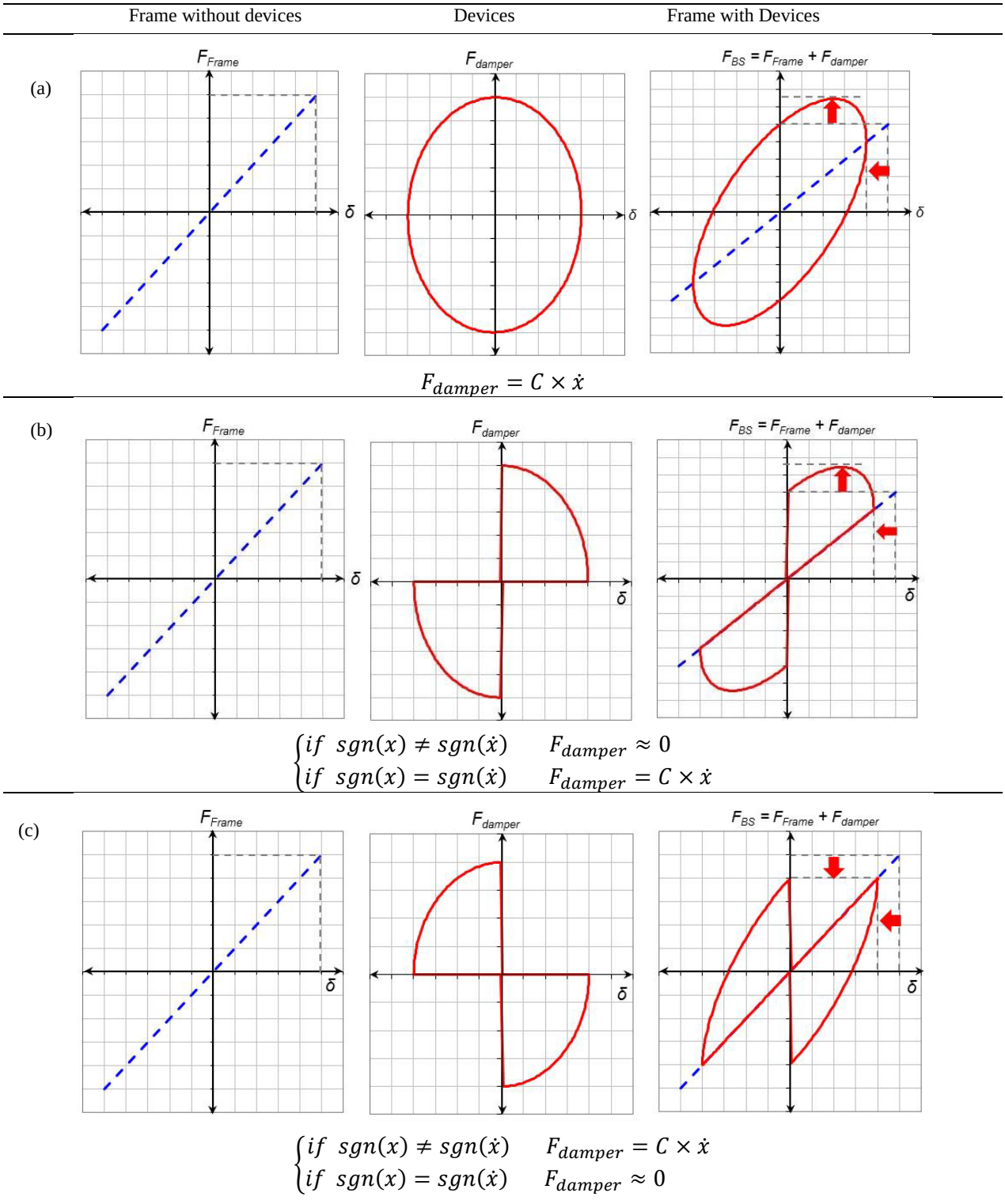

Figure 1: Schematic device hysteresis loop for a) 1-4 device, b) 1-3 device, and c) 2-4 device.

The prototype piston was constructed with 30 independent orifices of different sizes. These orifices have a range of sizes and can be individually blocked to experimentally test different configurations and damping levels. Figure 2 shows the dimensions and layout of orifices on the piston. Tests were done with three different orifice combinations (Figure 2):

- Case 1: 12× Ø4.5mm + 6× Ø3.5mm orifice open, total open orifice area= 994.3mm^2
- Case 2: 6× Ø3.5mm orifice open, total open orifice area= 230.9mm^2
- Case 3: 3× Ø3.5mm orifice open, total open orifice area=115.4mm^2

The main aim of having different orifice areas open is to characterize the viscous damping force obtained. As the piston moves at a given velocity, it dictates a flow rate that must pass through the open orifice area. This flow rate is equal to piston area multiplied by the velocity (mm/sec). A much higher fluid velocity through the orifices is required through orifices as their area is significantly smaller than the piston force area.

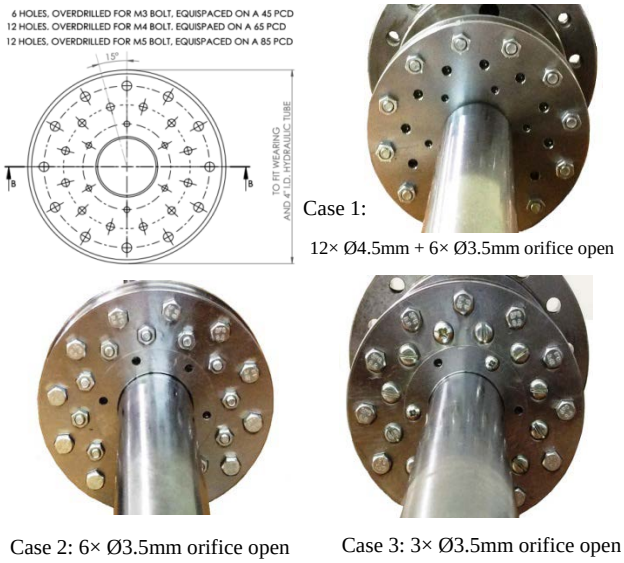

Figure 2: Geometry of piston showing the orifice orientation and case1 of orifice combinations. 18 orifices open (12× Ø4.5mm and 6× Ø3.5mm), 6 orifices open (6× Ø3.5mm) and 3 orifices open (3× Ø3.5mm).

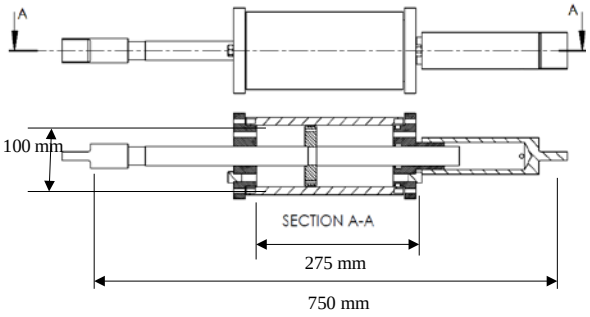

Figure 3: Model of damping device.

The end caps were fastened using 12×M8 hex socket bolts and sealed with an O-ring and back-up. Each end cap contained a threaded hole for a pressure sensor and a grub screw, which could be easily removed to add or remove oil. Both holes were sealed with thread tape and the use of copper washers. Figure 3 shows a schematic model of the damping prototype.

Linear viscous dampers are typically characterized by using sinusoidal test input and constitutive law where the force (F) is a function of velocity (v):

$$F = Cv \tag{1}$$

$$v_{\max} = 2\pi f A \tag{2}$$

where, C is a constant expressed in units of a force divided by a velocity (kN.s/m), v_{max} is maximum velocity, and f and A are frequency and amplitude of a sinusoidal excitation, respectively.

Figure 4 shows the hysteresis loop when 18 orifices are open (Case 1) under sinusoidal inputs with frequencies of 0.3 Hz to 0.9Hz and amplitude of 60mm. As expected increasing velocity with increasing frequency leads to larger forces. Table 1 shows good agreement between the maximum experimental velocities with values from Eq.1. Figure 4 also shows the relationship between analytical and experimental velocity, including saturation of velocity of the MTS machine at 340 mm/sec. Beyond this limit, the MTS hydraulic test machine did not have the flow rate required to accurately track the command displacement profile, leading to this velocity saturation. The saturation is thus a limitation in this specific test machine, not a problem with the viscous damper.

In particular, as the test machine reached maximum speed, it produces non-sinusoidal 'triangle waves' at a saturated constant velocity that also saturates device force, as shown in Figure 5.

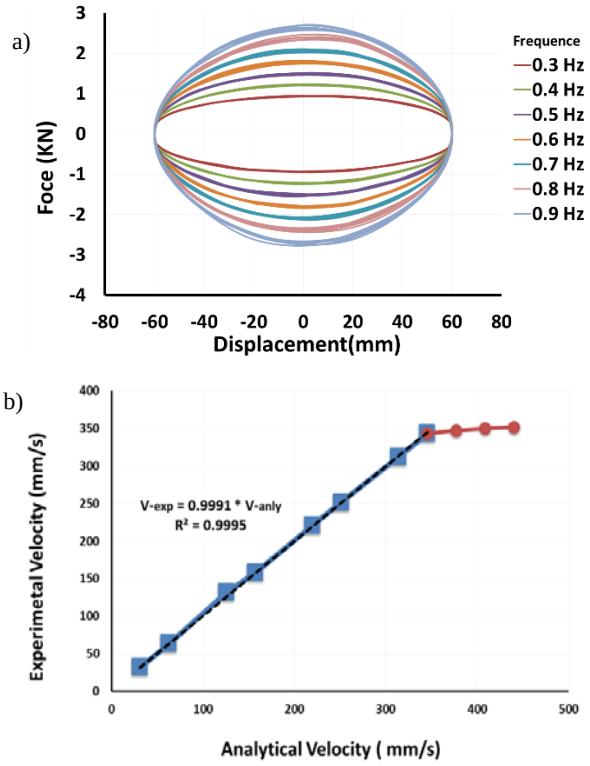

Figure 4: a) Force-displacement of the viscous damper with 18 orifices open under sinusoidal loading with different frequencies, b) Relationship between analytical and experimental velocity of the viscous damper with 18 orifices open.

Table 1: Compression between the maximum experimental velocities with analytical ones that calculated from Eq.1 of viscous damper with 18 orifices open.

Frequency (Hz)	Amplitude (mm)	Analytical Velocity (mm/s)	Experimental Velocity (mm/s)
0.25	20.00	31.42	31.73
0.50	20.00	62.83	63.28
1.00	20.00	125.66	131.36
1.25	20.00	157.08	157.67
1.75	20.00	219.91	220.74
2.00	20.00	251.33	251.44
2.50	20.00	314.16	312.22
2.75	20.00	345.58	343.26
3.00	20.00	376.99	347.00
3.25	20.00	408.41	350.50

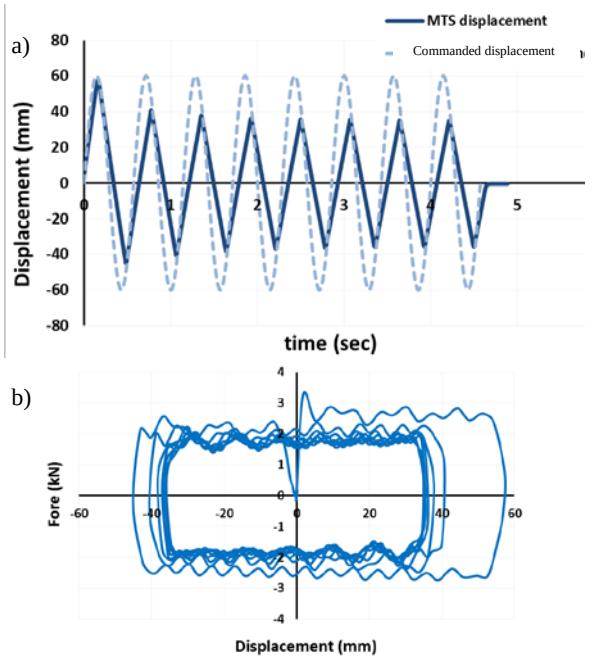

Figure 5: Results of the device under sinusoidal loading with frequency of 1.75Hz and amplitude of 60mm, (a) command input displacement and actual measured displacement (b) fore-displacement of the device.

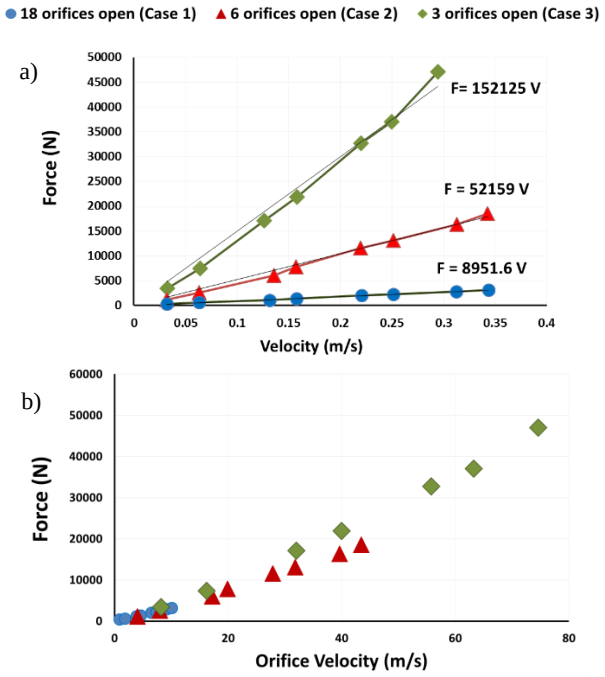

Figure 6: Maximum force and velocity of the viscous damper for all three cases. (b) Maximum force and orifice velocity for all three cases.

Figure 6 shows maximum force and velocity for all three cases. As expected, the maximum force increases with decreased open orifice area. The calculated damping, *C*, is approximately 152.5, 52 and 9kN.s/m for Cases 1, 2 and 3, respectively.

The velocity of flow through the orifices (v_o) is a function of piston velocity (v_p) and the ratio of the area of the piston (A_p) to the open orifice area (A_o):

$$v_o = v_p \frac{A_p}{A_o} \quad (3)$$

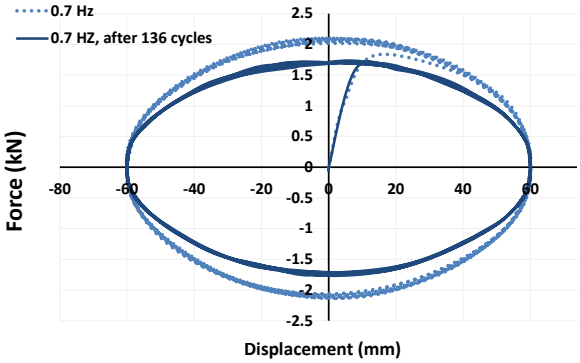

Figure 7: Force-displacement the viscous damper with 18 orifices opened under 0.7Hz sinusoidal load before and after a sequence of testing the included 136 cycles.

Figure 6b shows the maximum force versus orifice flow velocity for all three cases. The results indicate that the relationship between maximum force and orifice flow velocity has the same value for all of three cases, as expected since the assumption is a function of v_0 explicitly.

In a typical earthquake there are not many large, repeated cycles. The viscous damper does lose some portion of force due to heating when many input cycles are undertaken. Figure 7 presents the results for input amplitude of 30mm and a loading rate of 0.7Hz. Two sets of results are presented for the same input, one undertaken at the start of a sequence of testing, and the other at the end of a sequence of testing that comprised a total of 136 cycles across a time period of 12 minutes. The comparative results show a reduction in resistive force of approximately 17%. This loss of force is attributed to dynamic heating effects and the corresponding reduction in fluid viscosity, and would not be an issue in an earthquake where much fewer response cycles could be expected.

CREATING A PASSIVE SINGLE QUADRANT VISCOUS DAMPER

The damping device was modified in two steps, by first modifying the piston then by modifying the cylinder to have a passive single quadrant viscous damper. To provide one way flow and thus direction dependent damping, a flat ring plate was added to the piston design to cover the 12× 6mm orifices when the piston is moving toward the side with the ring. Three socket bolts are added on top of the flat ring to retain the washer and give the required space for moving of the plate (Figure 8). When moving in a direction with fluid pressure it on under side of the piston, the washer slides off the piston and open these larger outer orifices to allow increased fluid flow, reducing the damping force significantly. It should be noted that these retaining bolts are only one possible way of holding the circular ring in piston. The relation of this ring could also be obtained by a shoulder on the shaft or other similar method.

More specially, by adding the flat ring to the piston, there are two set of resisting forces dependent on the direction of the piston:

1. Large resisting forces: In one direction, with flow pressure against the ring, the fluid forces the ring plate to cover the longer outer ring of 12× Ø6mm orifices. Therefore the fluid is forced to flow through only the 6× Ø3.5mm orifices.
2. Low resisting forces: In the reverse direction when the flow moves through the 12× Ø6mm orifices, the plate lifts off the piston face allowing fluid flow through the longer orifices. Therefore, the orifices flow rate, V_0, drops substantially, as does the resulting damping force.

Figure 8: Scheme and photo of the modified piston.

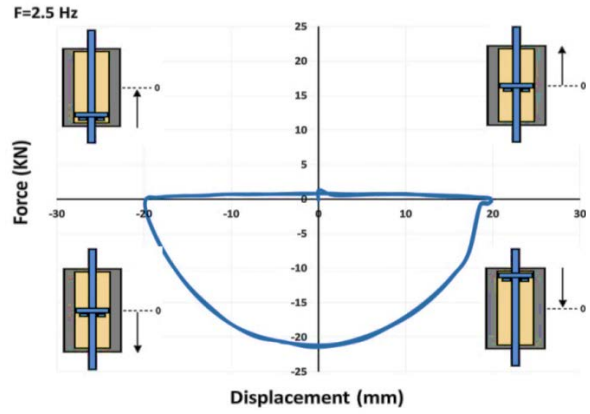

Figure 9: Force-displacement of the device showing half the hysteresis loop (2-3 quadrants only) of a viscous damper when 6 orifices are open under sinusoidal loading with frequency 2.5 Hz and amplitude 20 mm.

The modified piston alone produces a half hysteresis loop viscous damper. Figure 9 shows force-displacement of the device with the modified piston under sinusoidal loading with 2.5 Hz frequency and 20 mm amplitude. The damping forces are otherwise in line with those of Figure 6.

Figure 10 shows time delay of covering orifices by the flat ring plate. The device has a delay about 0.03s (from 0.81s to 0.84s in Figure 10c) until the flat ring covers the orifices. This delay should not have a significantly effect for most structures with typical fundamental frequencies in the 0.2-5.0Hz range. Some issue due to heating over many more large cycles than would be need in a typical earthquakes. However, silicone fluids may improve this behaviour using variants of silicone that have either Newton (linear Force-Velocity response) or Non-Newtonion (non-linear Force-Velocity) response. Future work could issue these trade-offs. The timing delay represents the time taken for a differential pressure to be established across the faces of the circular plate, causing it to be pushed against the piston face.

Figure 11 shows the hysteresis loops for 0.5Hz to 2.5Hz and an amplitude 20mm. Using the modified piston with one way valves provides direction dependent damping a half hysteresis loop of viscous damper. As in Figure 4, the maximum force increases with increasing velocity, as expected, just for half a cycle only.

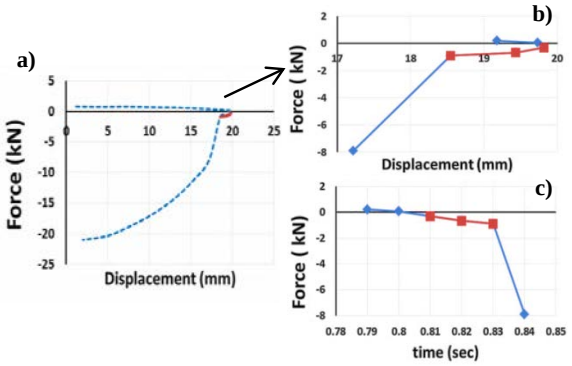

Figure 10: Time delay of covering orifices by the flat ring plate.

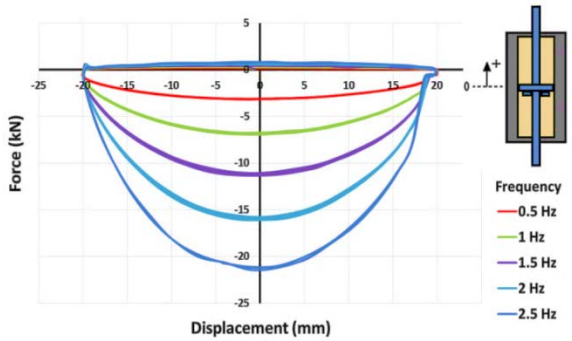

Figure 11: Force-displacement of the device that could have a half hysteresis loop of the viscous damper under sinusoidal loading with different frequencies and amplitude of 20 mm.

Figures 10-11 also show the time delay about 0.02 seconds, or less, covering motion of 1mm or less. This value is similar for all frequencies of input loading and is thus largely velocity independent. Here small values are due to the low inertia and friction of the washers used as valves in this instantiation and the influence of gravity. Alternative one-way valve configurations could be used to minimize this delay.

The next step is a device with damping in only one quadrant of the force-displacement plot. To achieve a single quadrant hysteresis loop, requires displacement or location dependent damping so that damping is only produced in one half of the device cylinder. To achieve this goal, the internal cylinder diameter is increased over half of the device, to enable the fluid to flow through an annular gap around the piston circumference in this half of the cylinder, negating any damping when moving in either direction. Therefore, when the piston is located in the area that has larger cylinder bare diameter the device produces only minimal damping forces. The design illustration is shown in Figure 12.

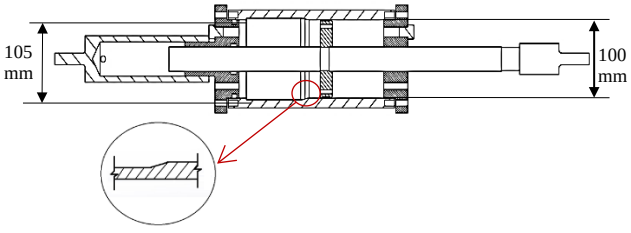

Figure 12: Scheme of the modified cylinder.

Step-by-step representation of piston position under a sinusoidal input for a single quadrant hysteresis loop is shown in Figure 13. Only in quadrant 2 when the piston goes downward, does the circular ring cover the 12× Ø4.5mm orifices and the piston is within the narrower bare section of the cylinder are larger damping forces produced . At all after times there is minimal damping as fluid can flow through the larger diameter orifices or through the annular gap around the piston circumstance. The result is an expected single quadrant damping device. Reversing the piston head and/ or cylinder can provide damping in any given quadrant.

More specifically, by changing the direction of the piston within the cylinder and the device, four shapes of single quadrant hysteresis loop can be achieved. Figure 14 shows four ways of assembling the device to capture only one quadrant of the hysteresis loop as an active viscous damper. Combining these four options provides the full hysteresis loop of the viscous damper. Figure 14 shows a few experimental hysteresis loops for each case with sinusoidal input. Figure 15 overlays these for inputs from 0.25Hz to 2.5Hz and amplitude of 20mm.

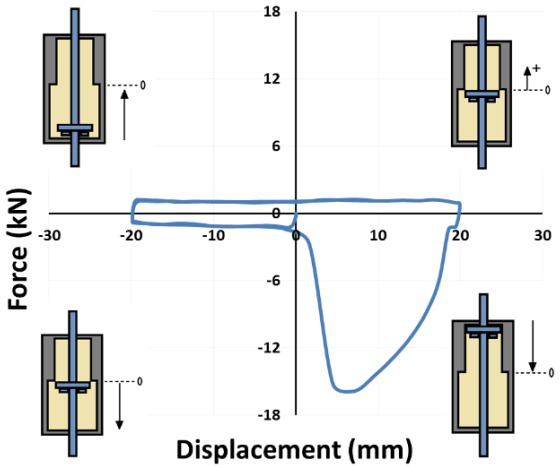

Figure 13: Step-by-step representation of position of the modified piston in the modified cylinder under a sinusoidal loading.

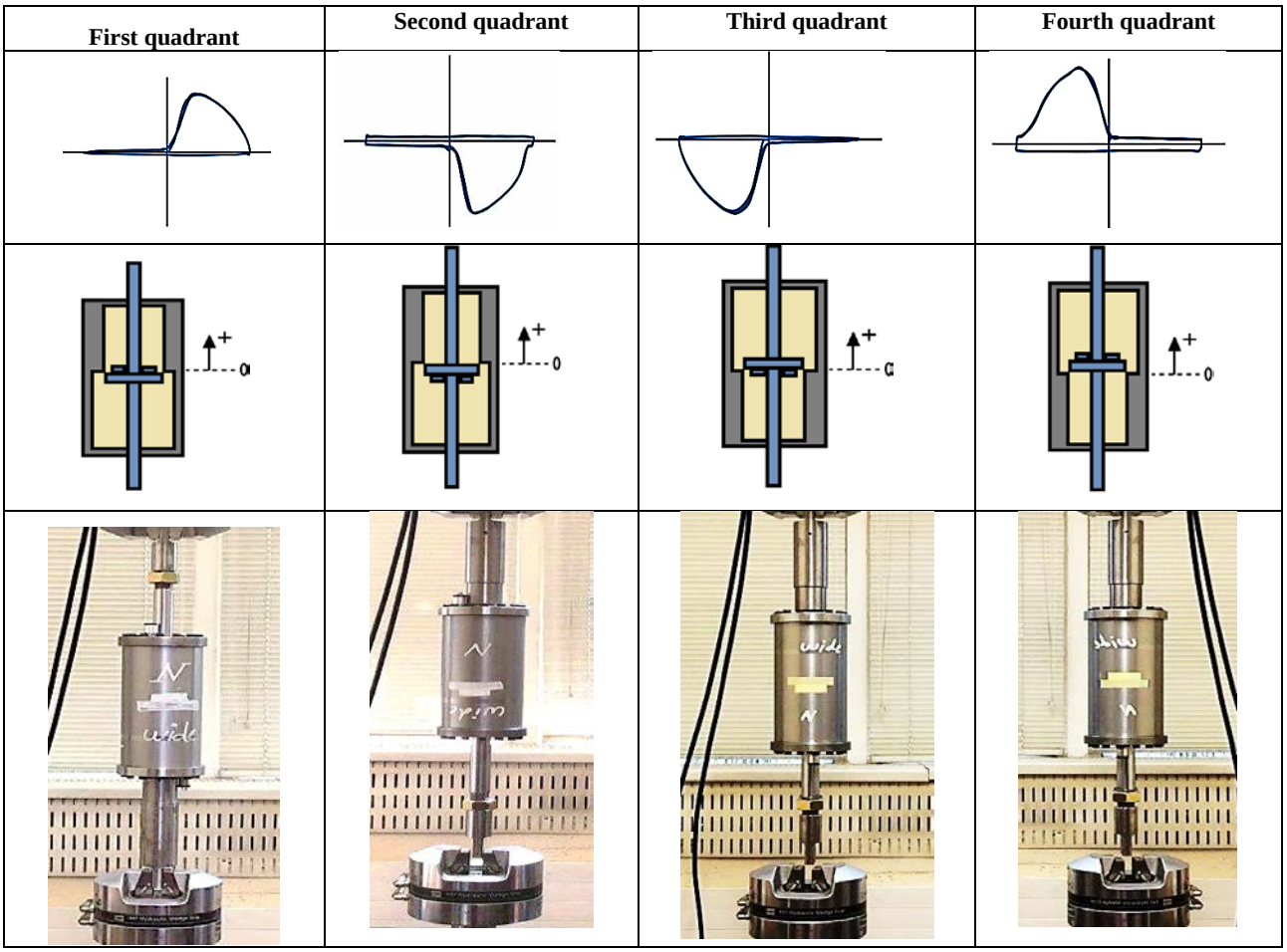

Figure 14: Four ways of assembling of the device to produce hysteresis loop in each of the four quadrants.

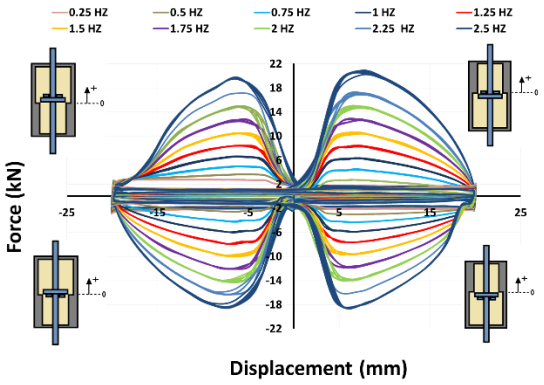

Figure 15: Force-displacement of four ways of assembling of the device under sinusoidal loading with range of frequency from 0.25Hz to 2.5Hz and amplitude of 20mm.

The low resistive force within 3-5mm of center line is due to the initial piston position and the slope transition between the narrow and wider sections of the cylinder. The cylinder can be designed so that there is an overlap into the next quadrant if desired. It is the transition shape and location that determines the shape and sharpness of this drop off. Results in Hazaveh et al. [16] for a 2-4 device show this difference clearly. Figure 1 also shows the device analytical equations. These equations are based on the linear, constant viscous damping coefficient found in Figure 6. The results in Figure 13 match this behaviour. However, as noted, the transition can vary with specific transition design in the cylinder.

Experimental test results of the 2-4 configuration of the resettable devices in prior work [8,9] and the proposed viscous device in the shake table tests [16] have showed that the change in the force displacement loop does not cause any major issues for the structure. Furthermore, the transition from the low-damping range to the high-damping range can be made more gradual if desired, to reduce the likelihood of any impulse forces being imparted into a structure.

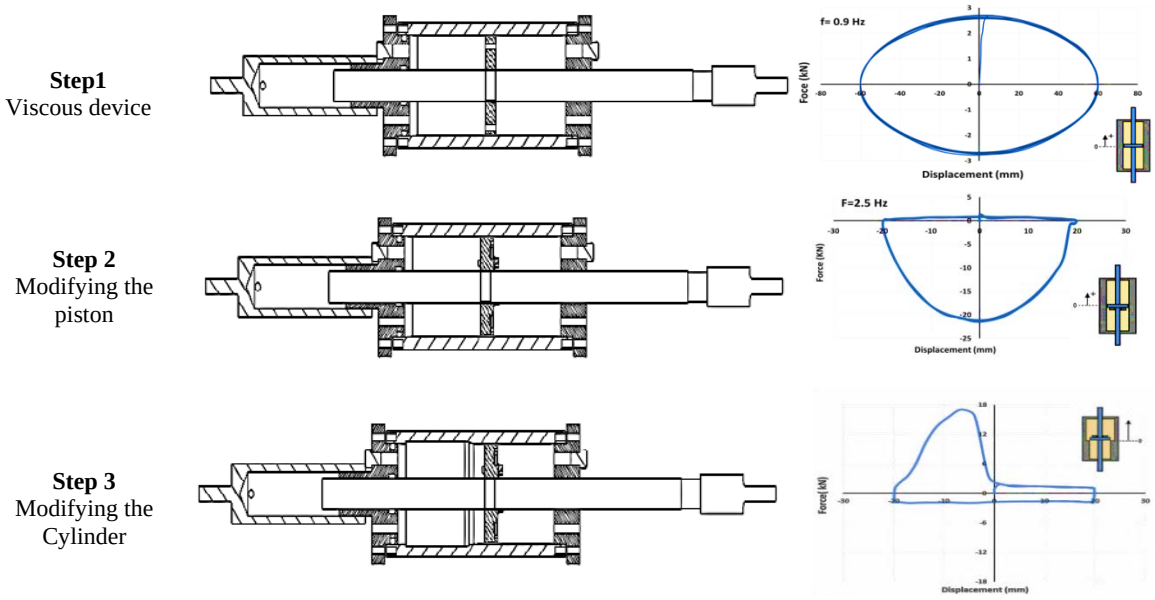

Figure 16: Modifying a typical viscous damper to capture a single quadrant hysteresis loop.

CONCLUSIONS

In this study the characteristic of a classic viscous damper are initially evaluated as a benchmark. This prototype viscous damper was then modified to achieve a passive Direction Dependent Dissipation (D3) device, which could add dissipation forces in any given quadrant of a hysteresis loop. Overall, this direction and displacement dependent damping behaviour could be used to generate a wide range of potential hysteresis loops that can be obtained by selecting individual quadrants, or parts of quadrants, where damping forces are produced. Therefore, the device could be tailored to provide a specific hysteresis loop to produce a desirable overall structural response. Experimental validation of a proposed device is undertaken using an MTS-810 hydraulic test machine under different sinusoidal loading. Both direction-dependence and position dependence have been individually investigated and validated. The experimental prototype D3 device tests confirm the capability of providing this direction dependent viscous damping in a relatively simple passive design with relatively low device cost.

ACKNOWLEDGMENTS

This project was (partially) supported by QuakeCoRE, a New Zealand Tertiary Education Commission-funded Centre. Funding from the NZSEE/EQC Ivan Skinner award, the BRANZ Building Research Levy, and the Natural Hazards Research Platform is also gratefully acknowledged. This is QuakeCoRE Publication number 0301.

REFERENCES

1 Amini F, Hazaveh NK and Rad AA (2013). "Wavelet PSO-Based LQR Algorithm for Optimal Structural Control Using Active Tuned Mass Dampers". *Computer-Aided Civil and Infrastructure Engineering*, **28**(7): 542-557.

2 Barroso LR, Chase JG and Hunt S (2003). "Resettable smart dampers for multi-level seismic hazard mitigation of steel moment frames". *Journal of Structural Control*, **10**(1): 41-58.

3 Chase JG, Mulligan KJ, Gue A, Alnot T, Rodgers G, Mander JB, Elliott R, Deam B, Cleeve L and Heaton D

(2006). "Re-shaping hysteretic behaviour using semi-active resettable device dampers". *Engineering Structures*, **28**(10): 1418-1429.

4 Feng MQ, Shinozuka M and Fujii S (1993). "Friction-controllable sliding isolation system". *Journal of Engineering Mechanics*, **119**(9): 1845-1864.

5 Hazaveh NK, Chase JG, Rodgers GW and Pampanin S (2015). "Smart semi-active MR damper to control the structural response". *Bulletin of the New Zealand Society for Earthquake Engineering*, **48**(4): 235-244.

6 Jabbari F and Bobrow JE (2002). "Vibration suppression with resettable device". *Journal of Engineering Mechanics*, **128**(9): 916-924.

7 Jansen LM and Dyke SJ (2000). "Semiactive control strategies for MR dampers: comparative study". *Journal of Engineering Mechanics*, **126**(8): 795-803.

8 Mulligan K, Chase J, Mander J, Rodgers G, Elliott R, Franco-Anaya R and Carr A (2009). "Experimental validation of semi-active resetable actuators in a ⅕th scale test structure". *Earthquake Engineering & Structural Dynamics*, **38**(4): 517-536.

9 Mulligan KJ, Chase JG, Mander JB, Rodgers GW and Elliott RB (2010). "Nonlinear models and validation for resetable device design and enhanced force capacity". *Structural Control and Health Monitoring*, **17**(3): 301-316.

10 Yoshida O and Dyke SJ (2004). "Seismic control of a nonlinear benchmark building using smart dampers". *Journal of Engineering Mechanics*, **130**(4): 386-392.

11 Rodgers GW, Mander JB, Geoffrey Chase J, Mulligan KJ, Deam BL and Carr A (2007). "Re-shaping hysteretic behaviour—spectral analysis and design equations for semi-active structures". *Earthquake Engineering & Structural Dynamics*, **36**(1): 77-100.

12 Hazaveh NK, Chase JG, Rodgers GW and Pampanin S (2015). "Control of Structural Response with a New Semi-Active Viscous Damping Device" *8th International Conference on Behavior of Steel Structures in Seismic Areas*, Shanghai, China.

13 Hazaveh NK, Pampanin S, Rodgers G and Chase J (2014). "Novel Semi-active Viscous Damping Device for Reshaping Structural Response". *Sixth World Conference of the International Association for Structural Control and Monitoring (6WCSCM)*, Barcelona, Spain.

14 Hazaveh NK, Rodgers GW, Chase JG and Pampanin S (2016). "Reshaping Structural Hysteresis Response with Semi-active Viscous Damping". *Bulletin of Earthquake Engineering* **15**: 1789-1806.

15 Hazaveh NK, Rodgers GW, Pampanin S and Chase JG (2016). "Damping reduction factors and code-based design equation for structures using semi-active viscous dampers". *Earthquake Engineering & Structural Dynamics*, **45**(15): 2533-2550.

16 Hazaveh NK, Rad AA, Rodgers GW, Chase JG, Pampanin S and Ma QT (2017)."Shake table test a structure retrofitted using 2-4 Direction Displacement Dependent (D3) viscous dampers". *NZSEE Annual Conference*,Wellington, NZ.